Mesoporous Silica Nanoparticles Functionalized with Hyaluronic Acid and Chitosan Biopolymers. Effect of Functionalization on Cell Internalization

Andrea Salis,[‡,] Maura Fanti,[†] Luca Medda,[‡] Valentina Nairi,[‡] Francesca Cugia,[‡] Marco Piludu,[†] Valeria Sogos,[†] and Maura Monduzzi[‡*]*

[‡] Department of Chemical and Geological Sciences, University of Cagliari-CSGI and CNBS, Cittadella Universitaria, S.S. 554 bivio Sestu, 09042- Monserrato (CA), Italy; [†] Department of Biomedical Sciences, University of Cagliari, Cittadella Universitaria, S.S. 554 bivio Sestu, 09042-Monserrato (CA), Italy.

*CORRESPONDING AUTHOR FOOTNOTE. Tel.: +39070675 4362/4385. Fax: +39 0706754388

Email: asalis@unica.it, monduzzi@unica.it;

ABSTRACT

Mesoporous silica nanoparticles (MSNs), based on the MCM-41 matrix, were functionalized with amino groups, and then with hyaluronic acid (HA) or chitosan (CHIT) to fabricate bioactive conjugates. The role of the functional groups towards cytotoxicity and cellular uptake was investigated using 3T3 mouse fibroblast cells. A very high biocompatibility of MSN-NH_2, MSN-HA and MSN-CHIT matrices was assessed through the MTS biological assay and Coulter counter evaluation. No significant differences in cytotoxicity data arise from the presence of different functional groups in the investigated MSNs. Fluorescence microscopy experiments performed using fluorescein isothiocyanate-conjugated MSN-NH_2, MSN-HA and MSN-CHIT, and transmission electron microscopy experiments performed on slices of the investigated systems embedded in epoxy resins give evidence of significant differences due to type of functionalization in terms of cellular uptake and stability of the particles in the biological medium. MSN-NH_2 and MSN-HA conjugates are easily internalized, being the uptake of the -HA functionalized much higher than that of the -NH_2 functionalized MSNs. Differently, MSN-CHIT conjugates tend to give large aggregates dispersed in the medium or localized at the external surface of the cell membranes. Both fluorescence microscopy and TEM images show that the MSNs are distributed in the cytoplasm of the cells in the case of MSN-NH_2 and MSN-HA, whereas only few particles are internalized in the case of MSN-CHIT. Flow cytometry experiments confirmed quantitatively the selectively high cellular uptake of MSN-HA particles.

Keywords: Nanomedicine; mesoporous silica nanoparticles; functionalization; biopolymers; hyaluronic acid; chitosan; cytotoxicity; transmission electron microscopy.

1. Introduction

Functionalization of materials is an art and has become a must in the development of smart nanodevices for a huge variety of applications, particularly in the challenging topics related to nanomedicine.[1–4] Indeed the design of a drug delivery formulation, and the fabrication of composite materials for either tissue engineering or theranostic, and stimuli responsive drug carriers, should carefully consider the nature of biological barriers. A favorable interaction between an external object and biological entities is addressed by bioadhesion processes which, at a nanoscopic level, can be regarded as a molecular recognition event. Therefore, as described by Gagner et al.[5], nanomaterials for biomedical applications require suitable functionalization to favor the interaction with the biomolecules. An increased awareness of the involvement of glycoproteins and oligosaccharides in many molecular recognition/inhibition biological processes has addressed the fabrication of bio-conjugates functionalized with saccharide biopolymers, proteins and peptides.[6,7] In this context several recent works have considered functionalized mesoporous silica nanoparticles (MSNs) as a very promising matrix to build a hybrid organic-inorganic bio-conjugate which can modulate weak, but very important, interactions that play significant roles in biology, those that occur when proteins bind to extracellular carbohydrates. Such protein-carbohydrate interactions are essential participants in many physiological cell-cell recognition processes, including fertilization, bacterial and viral pathogenesis, and the inflammatory response.[8–10]

Ordered mesoporous silica-based functional materials have raised great interest since their discovery in the nineties because of the easiness and the flexibility of the synthesis, the reproducibility of the texture, and of the morphology.[11] Besides the easy synthesis, other intrinsic peculiar features such as high surface area, uniform pore size distribution, high pore volume as well as the wide possibility to introduce functional groups have attracted an extraordinary interest on these materials.

In the last 20 years several different long-range ordered structures such as hexagonal, cubic or lamellar have been built.[12] Several research groups have produced interesting advances in the use of silica materials for nanomedicine applications.[1,2,4,13,14] Another interesting feature is the fact that the

silica-based ordered mesoporous materials display a high propensity to selectively adsorb proteins, peptides and enzymes.[15–17] This was clearly demonstrated through peculiar TEM experiments based either on a standard immunochemical method[18] or a silver enhancement procedure.[19]

In the last few years we have explored the peculiarities of ordered mesoporous materials to pursue a deep knowledge on the different interactions occurring between charged interfaces such as silica matrices and proteins. Particularly, we investigated the role of pH and ionic strength as well as specific electrolyte effects on the adsorption on, and the release from SBA-15 silica matrices of lysozyme.[15–17] Indeed proteins undergo dramatic specific ion effects in the presence of both weak (buffers) and strong electrolytes.[20–23] These findings highlighted the important role of weak and strong electrolytes when dealing with charged inorganic surfaces or proteins in relation to the complex nature of biological fluids. However, it should be remarked that non functionalized silica particles generally show very high toxicity, up to death, when injected *in vivo* via intravenous or intraperitoneal administration route.[24] Only subcutaneous injections were recognized as generally safe. Substantially, at present the use of MSNs is limited to the fabrication of drug depot systems or to bone regeneration treatments.[14,25–27] Remarkably, the role of biological fluids has not yet deeply been investigated. As emphasized by many authors[1,2,28–32] functionalization of MSNs constitutes a solid possibility not only for specific cell targeting but also for reducing toxicity and improving biodistribution.[33] To this aim functionalization based on bioactive moieties such as biopolymers and polyelectrolytes was shown to be a very promising choice.[34] Very recently we analyzed the adsorption of lysozyme on hyaluronic acid functionalized SBA-15.[35] The experimental findings suggested that a high level of functionalization of the silica surface almost prevents lysozyme adsorption whereas a low degree of functionalization of the silica allows for a large lysozyme adsorption. Interestingly, it was ascertained that during enzymatic degradation of HA-drug conjugated systems CD44 receptors favor the internalization of HA-conjugated nanoparticles by cells that enable intracellular delivery of drugs.[36–38] Focusing on functionalizations based on polysaccharides, it is worth mentioning that pH-responsive alginate/chitosan MSN conjugates allow

for drug release as pH decreases. This turned out to be very useful for tumor chemotherapeutics delivery both *in vitro* and *in vivo* experiments.[39] In addition, it was found that anticancer drugs loaded inside MSNs end-capped with chitosan can be released and internalized in tumor cells not only because of acidic pHs but also as a result of the high concentration of lysozyme, produced in large excess by cancer cells.[40] Indeed chitosan is easily hydrolyzed into monomers either by acidic pHs or by the catalytic activity of lysozyme, afterwards the drug can be released. In that case a dual stimuli-responsive drug carrier was fabricated.

This work focuses on MSNs based on MCM-41 matrices functionalized either with hyaluronic acid (HA) or chitosan (CHIT) and on the evaluation of their cytotoxicity towards 3T3 mouse fibroblast cell lines. As reported in recent works,[41–43] the functionalization with HA and CHIT should produce MSNs characterized by negative and positive charged interfaces respectively, at physiological pHs. However it should be remarked that many changes can occur when particles get in contact with biological environments. Particularly, the role of the composition of the growing media for cell proliferation on the particle surface charge can become a very complex task. Indeed, here we will demonstrate that cell internalization of functionalized MSNs strongly depends on the type of functionalization. In this context it is worth citing a recent paper by Treccani et al.[44] where the interaction between biological fluids and charged particles was carefully investigated.

2. Materials and Methods

2.1 Chemicals

Tetraethoxysilane (TEOS, 98%), hexadecyltrimethylammonium bromide (CTAB, > 99 %), anhydrous toluene (99.8 %), 3-aminopropyl-triethoxysilane (APTES, > 98 %), triethylamine (> 99 %), hyaluronic acid sodium salt from *Streptococcus equi* (cod. 53747), chitosan (cod. 740063, MW 60-120 kDa), NaH_2PO_4 (99 %), Na_2HPO_4 (99 %), fluorescein isothiocyanate (FITC) were purchased from Sigma-Aldrich (Milan, Italy). *N*-hydroxysuccinimide (NHS, > 97 %), and *N*-(3-dimethylaminopropyl)-*N′*-ethylcarbodiimide hydrochloride (EDC, > 98 %) were purchased from

Fluka. 3T3 were cultured in complete medium: DMEM (#6429,Sigma-Aldrich) supplemented with 10% fetal bovine serum (#F6178,Sigma-Aldrich), 1 μM L-glutamine (#G7513,Sigma-Aldrich), 100 U/mL penicillin and 100 μg/mL streptomycin (#4333,Sigma-Aldrich). MTS: CellTiter 96® AQueous One Solution Reagent (#G3581, Promega).

2.2 Synthesis of Mesoporous Silica Nanoparticles (MSNs).

1g of CTAB was dissolved in 480 g of Millipore water at room temperature by using an overhead stirrer. A volume of 3.5 mL of NaOH (2 M) was added to the surfactant solution, the temperature was then increased at 80°C and, after 2 h, 6.7 mL of TEOS were added drop wise. The solution was stirred for other 2 h and then the resultant white precipitate was collected by vacuum filtration and dried overnight at room temperature. The removal of CTAB surfactant was carried out by weighing 1.0 g of the synthesized material and adding 100 mL of a methanolic solution with 0.75 mL hydrochloric acid (37%) and stirring for 6 h at 50 °C. The mesoporous silica nanoparticles (MSNs) were then recovered via filtration and dried under vacuum at room temperature.[45,46] The grafting of the amino group on the surface of the MSNs was carried out by dispersing 1 g of the sample in 30 mL of anhydrous toluene and then by adding dropwise 1.0 mL of APTES. The dispersion was heated under reflux for 15 h. The resulting MSN-NH_2 sample was collected by filtration, washed with acetone, and dried overnight at room temperature under vacuum.

2.3 Functionalization and characterization of MSN-NH_2 particles

2.3.1 Functionalization of MSNs with Hyaluronic Acid (HA). A mass of 100 mg of MSN-NH_2 sample was dispersed in 100 mL of millipore water. In another reaction vessel, 20 mL of an aqueous solution containing NHS (0.37 g) and EDC (0.2 g) was mixed with 60 mL of an aqueous solution containing 113 mg of HA. The two solutions were mixed and the pH was adjusted to 9.0 by adding triethylamine. Finally, the mixture was stirred at 38°C overnight. The HA-modified MSNs (MSN-

HA) were collected after centrifugation, three washings with millipore water, and dried under vacuum and at room temperature overnight.[34]

2.3.2 Functionalization of MSNs with chitosan (CHIT). Chitosan has a free aminogroup per unit of sugar. The grafting of the chitosan biopolymer to MSN-NH_2 was achieved by linking the amino groups of both the biopolymer and the particles with glutaraldehyde bifunctional reagent. 0.1g of MSN-NH_2 sample were soaked for 1 h in a solution composed by 100 µL of aqueous glutaraldehyde (50%) and 2.5 mL of 0.1 M phosphate buffer solution (pH 7.5). The activated material was washed for three times under stirring with the same buffer (2.5 mL), centrifuged and the supernatant was removed through a Pasteur pipette. The MSN-NH_2 dispersion was then mixed with a suspension of chitosan containing 50 mg of chitosan in 2.5 mL of 0.1 M buffer solution at pH 8. The mixture was gently stirred overnight at 25°C and then the material was collected by filtration and washed with a slightly acid buffer solution (pH = 6) to remove the excess of chitosan. The material was dried under vacuum and at room temperature overnight.

2.3.3 Labelling of MSN-NH_2, MSN-HA, and MSN-CHIT with FITC. A mass of 20 mg of MSNs (MSN-NH_2, MSN-HA, MSN-CHIT) was suspended in 3 mL of millipore water, and mixed with 5 mL of a 0.3 mg/mL FITC ethanol solution. The suspension was stirred at room temperature in dark conditions for 6h and the particles were centrifuged, then washed three times with ethanol. The FITC labelled particles were used for fluorescence microscope observations and flow cytofluorimetry.[34]

2.3.4 Physico-chemical characterization of functionalized MSNs. Thermogravimetric analysis (TGA) was carried out on a Mettler-Toledo TGA/STDA 851. Thermal analysis data were collected in the 25−1000 °C range, under oxygen flow (heating rate = 10 °C·min^{-1}; flow rate = 50 mL·min^{-1}). The hydrodynamic diameter and the zeta potential of MSNs were measured using a Zetasizer nano ZSP (Malvern Instruments) in backscatter configuration (θ =173°) at laser wavelength of λ = 633 nm. The scattering cell temperature was fixed at 37°C and the data were analyzed with the Zetasizer software 7.03 version. For both zeta potential and DLS measurements the sample was prepared by

suspending MSNs (1 mg/mL) in filtered (0.2 μm polypropylene filter, Whatman) milliQ water. Samples were sonicated for 30 min and left under agitation overnight. Samples were sonicated for other 30 min and then the measurements were carried out.

2.4 Biological methods

2.4.1 In vitro viability assay. Cytotoxicity of MSNs was determined by the MTS assay. 3T3 mouse fibroblast cells were cultured in complete medium at 37°C in a 5% CO_2 humidified environment. 3T3 cells were plated at a density of 3x105/mL in 96-well plates for 24 hours, and then incubated with serial concentrations of MSN-NH_2, MSN-HA, and MSN-CHIT (from 200 μg/mL to 6.2 μg/mL), (t=0). After 24 hours, MSNs were removed and replaced with fresh complete medium. Cell viability was quantified by adding 20 μL of Cell-Titer 96 Aqueous One Solution Reagent (MTS) to the cultures for 2 hours at 37°C, immediately (t = 24h), then after 24 (t =24h+24h) and 48 (t = 24h+48h) hours after MSNs removal. Samples were read at λ = 490 nm for colorimetric assessment. All the experiments were performed at least in triplicate for each group.

2.4.2 Cell growth curve. 3T3 cells were plated 4x104/mL in 12-well plates. The day after (t=0) cells were treated with 100 μg/mL of MSNs for the analysis of cell growth. After 24 hours MSNs (MSN-NH_2, MSN-HA, and MSN-CHIT) were removed, and cells were cultured with fresh medium. Cell counts were performed immediately (t = 24h), then after 24 (t =24h+24h) and 48 (t = 24h+48h) hours after MSNs removal, using a Beckman Coulter counter. All the experiments were performed at least in triplicate for each group.

2.4.3 Intracellular uptake through fluorescence microscopy. 3T3 cells were plated at a density of $3x10^5$/mL on glass coverslips. After 24 hours from seeding, cells were incubated with 100 μg/mL FITC-labeled MSN-NH_2, MSN-HA, and MSN-CHIT for 24 hours. After treatment, MSNs were removed and cells maintained in fresh complete medium for further 24 hours. Then, cells were washed with PBS, stained for 30 minutes with Hoechst dye 33342 for nuclei, and observed using an

Olympus BX41 fluorescence microscope equipped with an appropriate filter for FITC detection (λ_{Ex}= 490 nm; λ_{Em}= 517 nm).

2.4.4 Intracellular uptake through flow cytometry. 3T3 cells, after treatment with FITC-labeled MSNs as described above, were dissociated by 0.25% trypsin/EDTA and resuspended in PBS. MSN uptake was analyzed using a BD FACSCANTO II flow cytometer (Becton Dickinson Biosciences, CA). At least 10,000 cells were analyzed in each sample. Cells without nanoparticle treatment were used as controls.

2.5 Transmission Electron Microscopy

Samples of 3T3 cells were treated with 100 μg/mL of MSN-NH_2, MSN-HA, and MSN-CHIT for 24 hours. After treatment, MSNs were removed and cells maintained in fresh complete medium for further 24 hours. Then, cells were fixed for 2 hours in a mixture of 1%(para)formaldehyde (Electron Microscopy Sciences) and 1.25% glutaraldehyde (Electron Microscopy Sciences) in 0.1 M sodium cacodylate (Electron Microscopy Sciences) buffer (pH 7.4). Cells were rinsed in the same buffer after fixation, postfixed in 1% osmium tetroxide for 1h and finally stained in aqueous uranyl acetate 0.25% overnight at 4°C. The next day the cells were processed by standard methods for embedding in epoxy resin.[47] In detail they were dehydrated in a graded series of ethanol and xylene and infiltrated overnight in Epon 812/xylene mixtures at room temperature. Cells were finally embedded in pure Epon 812 resin, transferred to dry beam capsules or flat embedding molds previously filled with embedding medium and polymerized in a oven at 60°C for 24 hours. Embedded cells were trimmed and sectioned after the resin blocks returned to room temperature. Ultrathin sections of the above samples (60-90 nm thick) were cut with a LKB ultratome 8800 ultramicrotome and collected on formvar-coated grids. They were post-stained with uranyl acetate and bismuth subnitrate, washed three times with distilled water and finally observed and photographed in a transmission electron microscope (JEOL 100S model, Tokyo, Japan) operating at 80 kV.

3. Results

3.1 Characterization of functionalized MSNs

Mesoporous silica nanoparticles (MSNs) were synthesized according to Yu et al.[34] A detailed characterization of MSN is reported in Figure S1 in the supporting information file. It includes the textural characterization (Figure S1A-B) obtained by the nitrogen adsorption/desorption isotherms which allowed to measure the surface area (S_{BET} = 1193 m^2/g), pore volume (V_p = 0.87 cm^3/g) and the maximum of pore size distribution (d_p = 22 Å). The structural characterization was carried out by means of small angle X-rays scattering (Figure S1C) and transmission electron microscopy (Figure S1D). Both techniques confirm the occurrence of the hexagonal array of pores the synthesized MSNs. Additionally, the TEM image in Figure S1D allows to estimate a particle size in the range 100–130 nm.

Scheme 1 summarizes the steps involved in the functionalization of MSNs. A reaction with aminopropyltriethoxysilane (APTES) introduces the amino group on the surface. This group is needed for the subsequent functionalization steps with hyaluronic acid (HA) and chitosan (CHIT) respectively. HA binding requires the use of two additional reagents, namely NHS and EDC.[35] CHIT binding was carried out similarly to what currently done in the covalent immobilization of enzymes on solid supports[49] using glutaraldehyde, a bifunctional reagent, which is able to react with the amino groups of MSN-NH_2 and those of chitosan biopolymer.

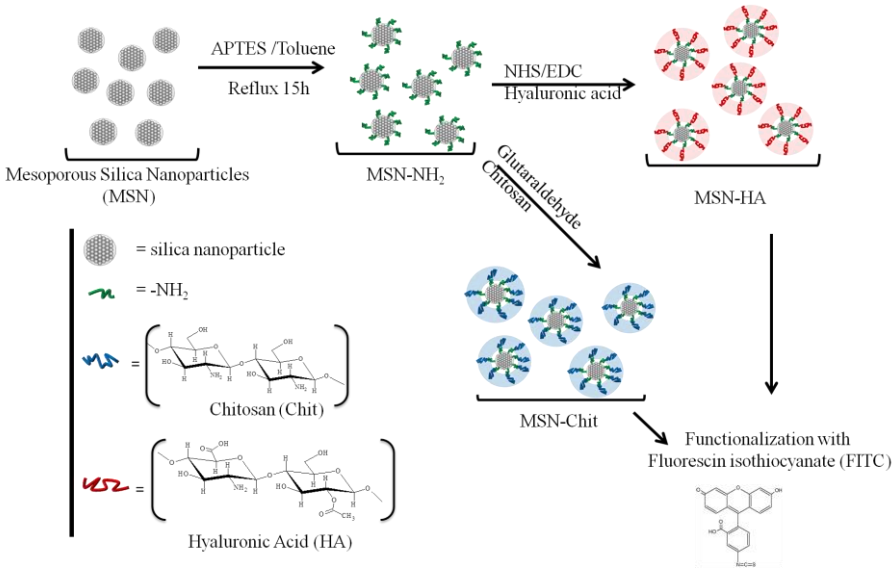

Scheme 1. Steps involved in the functionalization of mesoporous silica nanoparticles (MSNs) to obtain amino- (MSN-NH_2), hyaluronic acid- (MSN-HA), chitosan- (MSN-CHIT) and fluorescin isothiocyanate- mesoporous silica nanoparticles.

Functionalization of MSNs was proved by means of thermogravimetric analysis (TGA). Figure 1 compares the percentage mass loss profiles as a function of temperature for functionalized MSNs.

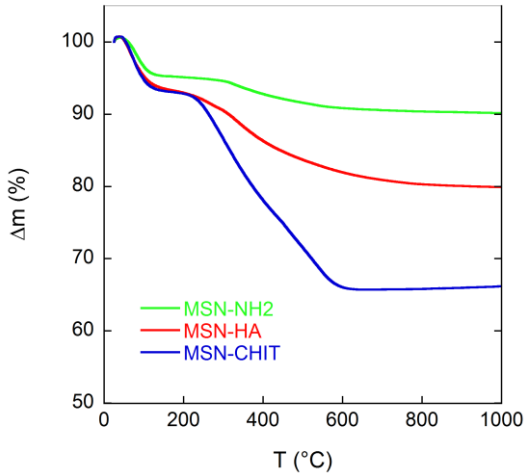

Figure 1. Percentage mass loss profiles as a function of temperature for functionalized MSNs (MSN-NH_2, MSN-HA, and MSN-CHIT).

The values of partial mass loss below and above 200 °C are reported in Table 1. For temperatures below 200 °C, a mass loss of 4.9% is obtained for MSN-NH_2 particles. This mass loss can be ascribed to the removal of humidity and to the condensation of surface silanols. Above 200 °C the mass loss is due to the burning of organic groups. At T > 200 °C a Δm = 5.0%, is obtained for MSN-NH_2. The functionalization with HA produces mass loss of about 7% for both MSN-HA and MSN-

CHIT at T<200°C. Instead, at T>200°C Δm is 13.1% for MSN-HA and of 26.7% for MSN-CHIT, respectively. The higher mass loss found for MSN-CHIT respect to MSN-HA suggests that the former sample has a higher degree of grafted biopolymer compared to the latter.

Additional characterization of the functionalized samples was carried out through FTIR spectroscopy. Figure S2 compares the FTIR spectra of MSN-NH_2 with those of MSN-HA and MSN-CHIT and the text in supporting information gives a description of band assignment. Substantially, TGA and FTIR techniques confirm the success of the functionalization procedure.

Table 1. Characterization of functionalized MSNs by means of TGA (Δm%), zeta potential (ζ) and hydrodynamic diameter (d_H).

	TGA (Δm %)		**MilliQ water**		**Cell culture medium**	
Sample	**<200 °C**	**>200°C**	**ζ (mV)**	**d_H (nm)-Number**	**ζ (mV)**	**d_H (nm)-Number**
MSN-NH_2	4.9	5.0	9.7±0.8	126±2	-11.3±0.6	131±2
MSN-HA	7.0	13.1	-7.2±0.8	156±3	-10±1	138±1
MSN-CHIT	7.1	26.7	40±1	169±3	-6.7±0.9	157±4

These functionalizations are expected to produce differently charged MSNs. Particularly once dispersed in an aqueous medium, positive charges for MSN-NH_2 and MSN-CHIT, and negative charges for MSN-HA surfaces would occur. This was confirmed by zeta potential measurements (Table 1). Indeed the values of ζ are positive (9.7±0.8 mV) for MSN-NH_2 but changes sign after functionalization with HA (-7.2±0.8 mV). Finally, the functionalization with positively charged polymer chitosan makes the nanoparticles even more positively charged (40±1 mV). This would result in a very highly stable suspension in distilled water. Similar measurements carried out using the cell culture medium as particle dispersant. This was done since one of the main aims of the work was the evaluation of the interactions between the different MSNs and the 3T3 mouse fibroblast cells. Thus, functionalized MSNs were prepared using the cell culture broth as dispersing medium. This medium is constituted by high glucose DMEM, 10 v% Fetal Bovine Serum and 0.5 v% antibiotics, and any attempt to measure the zeta potential of our MSNs failed: both medium and MSNs, independently of the functionalization, gave a zeta potential around -10 mV as already

observed by Treccani et al.[44] These findings are clearly related to the complexity of the culture medium, particularly to the high ionic strength and to the presence of DMEM amino acids and FBS proteins which can adsorb at the particle surface and, eventually, form a protein corona.[31,44]

The functionalized particles were characterized with dynamic light scattering for the determination of the hydrodynamic diameter, d_H, (Table 1 and also Figure S3 in Supporting Information) both in MilliQ water and cell culture medium. In MilliQ water, the size (d_H) of MSN-NH_2 is 126±2 nm and becomes 156±3 nm (MSN-HA) and 169±3 nm (MSN-CHIT) after biopolymer functionalization. This size increase is consistent with a successful functionalization of mesoporous silica nanoparticles. In the cell culture medium, the size of the MSNs is not significantly different for MSN-NH_2, whereas it is slightly lower for MSN-CHIT (157±4 nm) and even lower for MSN-HA (138±1 nm). A possible of explanation is that the electrolytes occurring in the culture medium, besides to affect the measured zeta potential, also play a role to decrease the hydrodynamic diameter of the biopolymer-functionalized MSNs.

Figure 2 shows the TEM images at low magnification of the functionalized MSNs. We observe that there is a good correspondence, at least at qualitative level, between particle sizes obtained with DLS and TEM techniques.

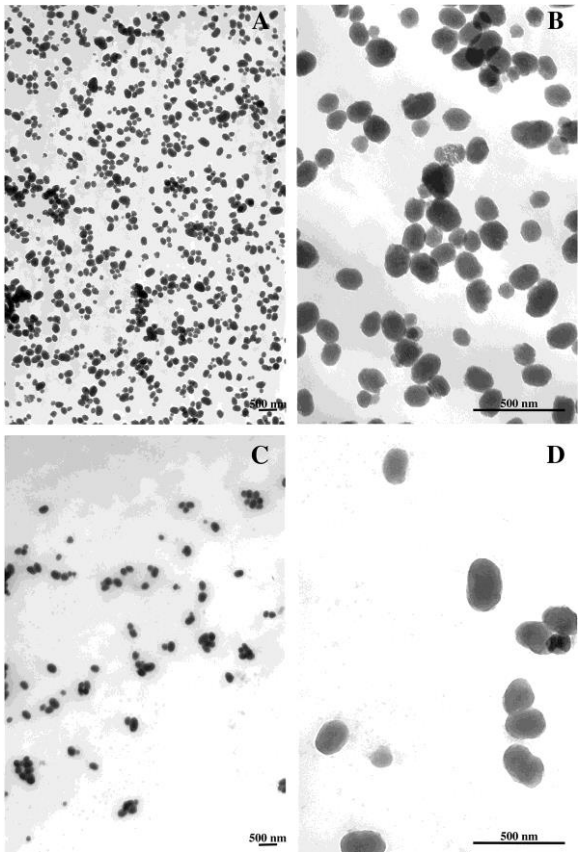

Figure 2. TEM images of functionalized MSNs. A,B) MSN-HA; C,D) MSN-CHIT.

In order to improve the ultrastructural details of functionalized particles by standard transmission electron microscopic techniques, we have treated nanoparticles with phosphotungstic acid solution. To date, the phosphotungstic acid staining is a rapid and easy method employed during electron microscopic investigations of isolated particles,[50] virus,[51] and organelles,[52] that usually appear brilliant in a amorphous electron-dense layer. As negative staining, it mainly allows the analysis of the superficial details of nanoparticles and individual macromolecules at electron microscopy level.

After treatment with phosphotungstic acid solution we observed the presence of an electron lucent halo surrounding the MSN-HA and the MSN-CHIT particles (Figure S4). That halo was not observed for MSN-NH_2. Although the nature of the electron lucent halo detected on the above particles needs to be completely ascertained by additional and more specific EM counterstaining techniques, its presence could be ascribed to the HA and CHIT functionalization processes respectively.

3.2 Cell viability and Counts

The effect of MSNs on 3T3 cell viability and proliferation profiles were evaluated using MTS assay and Coulter counter assay. Cell viability was measured after exposure to different concentrations of MSN-NH_2, MSN-HA, or MSN-CHIT for 24 hours. Figure 3 shows the viability measured with respect to controls (%) for concentrations of MSNs up to 200 µg/mL. Figure 3A shows the viability determined immediately after MSNs removal. Figures 3B and 3C show the viability measured after MSNs removal for 3T3 cells allowed to grow in the medium for other 24 or 48 hours, respectively. The experiments performed immediately after MSNs removal show a small decrease of viability with the lowest concentrations of MSNs (Figure 3A). On the contrary, no decrease of cell viability was observed for experiments carried out after 24 or 48 hours (Figures 3B-C).

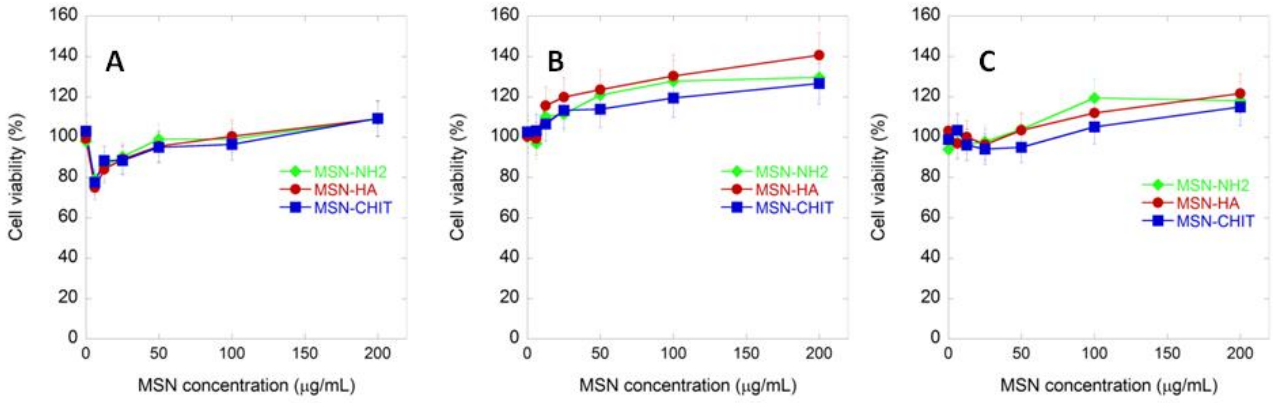

Figure 3. Effect of MSN-NH_2, MSN-HA, and MSN-CHIT on the viability/proliferation of 3T3 cell line incubated with the different MSNs for 24 hours. Viability measurement through MTS assay: A) immediately after MSNs removal; B) 24 hours after MSNs removal, and C) 48 hours after MSNs removal according to the protocol in par. 2.4.1.Values are expressed as percentage of control wells containing culture medium without MSNs. Results represent the mean ± standard deviation of three independent experiments.

In addition, we note that viability measured for MSNs concentration of 200 µg/mL becomes very high compared to control, particularly for MSN-HA 24 h after MSNs removal (Figure 3B), and for all MSNs when cells are left to grow in the medium for 48 hours after MSNs removal (Figure 3C). We can suggest that MTS assays are commonly used, and certainly reliable in relation to the evaluation of biocompatibility, but more at a qualitative rather than at a quantitative level. However these findings confirm the good safety of MSNs used in this study towards 3T3 fibroblast cells.

Indeed, it has been suggested that the presence of inorganic objects such as our MSNs (particles internalized or located on the cell membranes), may originate interference with the colorimetric assay as observed by Bancos et al.[53] Clearly the MTS assay can prove the general viability but, at a quantitative level, cell counts are more reliable. The experiments of cell counts were performed using the same conditions used for MTS assay in terms of contact time and following measurements. The MSNs concentration of 100 µg/mL was considered. Figure 4 shows the results of cell counts obtained for the different MSNs compared to the control. All measurements were performed in triplicate, and the quantitative results demonstrate again the safety of our MSNs, and also the fact that the highest growing speed of the cells is observed when cells are left to grow for 24 h after the incubation with MSNs. It is remarkable that both cytotoxycity and cell proliferation are not influenced by the type of functionalization of the MSNs.

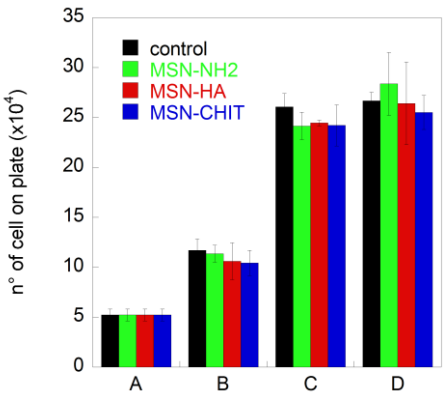

Figure 4. Effect of MSN-NH_2, MSN-HA, MSN-CHIT, and controls on the proliferation capacity of 3T3 cell line incubated with the different MSNs for 24 hours, and then left in contact with the culture medium for different times. Cell count: A) number of cells before treatment (t=0); B) number of cells immediately after MSNs removal (t = 24h); C) number of cells 24 hours after MSNs removal (t = 24h+24h); D) number of cells 48 hours after MSNs removal (t = 24h+48h) according to protocol in par. 2.4.2

3.3 Intracellular uptake. The cellular uptake performance of the MSNs was visualized by fluorescence and transmission electron microscopes. Figure 5 shows the fluorescence microscopy panels of 3T3 cells incubated with the FITC-labeled MSNs for 24 hours, afterwards MSNs were removed, and cells were left to grow in the culture medium for 24 hours before performing the

fluorescence microscopy analysis. Differently from the proliferation experiments, the cellular uptake performance depends significantly on MSN functionalization.

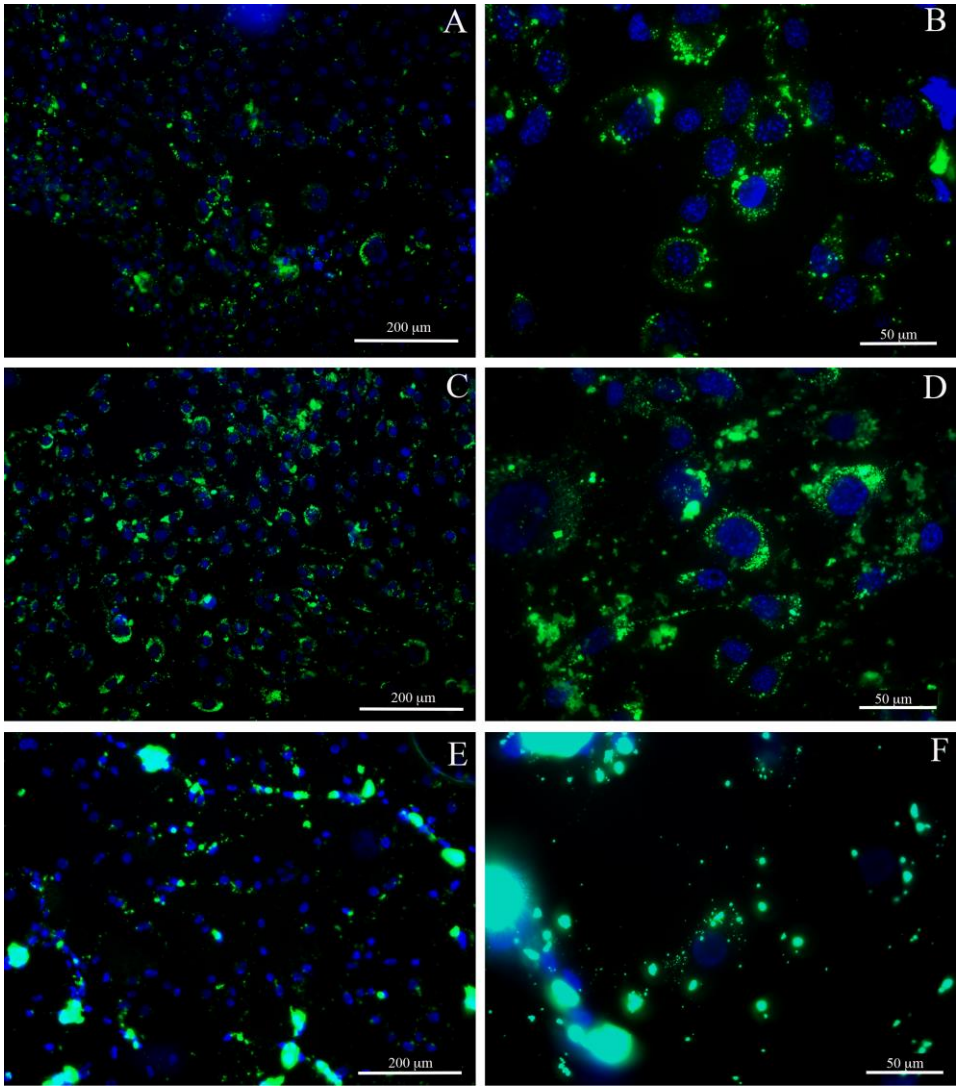

Figure 5. Internalization of MSNs using fluorescence microscopy. Images at different magnification (bars: left side 200 µm, right side 50 µm) of 3T3 mouse fibroblasts incubated for 24 hours with 100 µg/mL of MSNs, and then left to grow for other 24 hours in the culture medium (see par. 2.4.3). Panel A-B: MSN-NH_2, Panel C-D: MSN-HA, Panel E-F: MSN-CHIT. Blue: nuclei (Hoechst assay); green fluorescence: FITC-MSNs.

Indeed, we observed that about half of the cells incubated with FITC-MSN-NH_2 display significant amounts of internalized MSNs (Figure 5A, B), almost all the cells incubated with FITC-MSN-HA display high amounts of MSNs in their cytoplasm (Figure 5C, D), whereas only few cells incubated with FITC-MSN-CHIT show a very low number of internalized MSNs (Figure 5E, F). Indeed FITC-

MSN-CHIT nanoparticles tend to form large aggregates outside or over the cells as demonstrated by the presence of big fluorescent spots in Figure 5 E and 5F.

The qualitative observations of fluorescence microscopy were supported by flow cytometry analysis that determined the cellular uptake of FITC-MSNs into 3T3 cells by the incorporated fluorescence intensity. Figure 6 shows representative flow cytometry assessment of controls cells and cells treated with FITC-MSN-HA, indicating a very efficient uptake of nanoparticles. FITC-MSN-HA were efficiently internalized by all the cells, whereas the uptake of FITC-MSN-NH_2 was lower, since about 79% of cells were FITC positive. Finally, the uptake of MSN-CHIT is not shown since unreliable results due to the formation of big aggregates into the cell culture medium were obtained. However, this behavior is consistent with what observed in Figure 5E-F.

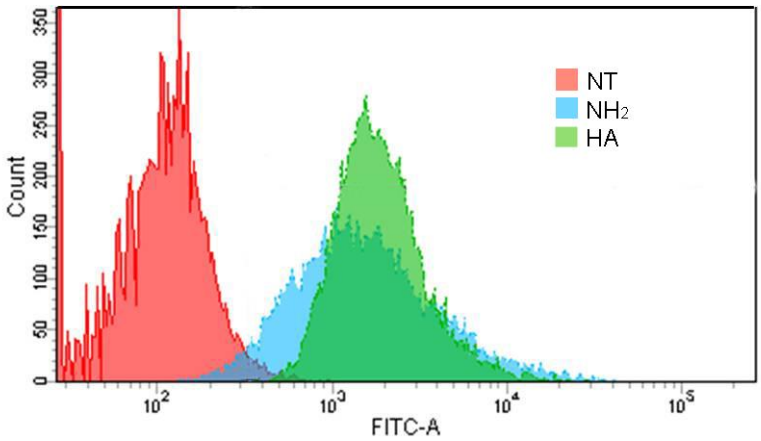

Figure 6. Flow Cytometry (G): Histogram plot of control cells (red) and cells incubated with FITC-labeled MSN-NH_2 (blue) or MSN-HA (green).

3.4 Electronic microscopy

Electron microscopy analysis confirmed and extended the results obtained by means of fluorescence microscopy. TEM highlighted at ultrastructural level significant differences in the morphological events that occurred in 3T3 cell cultures after exposure to the different types of functionalized MSNs. Figure 7 shows some significant TEM images (see also Figure S5 in Supporting Information). In detail, 3T3 cells following MSN-NH_2 treatment exhibited only few cytoplasmic vesicles containing MSN particles (Figure 7 A,B). Differently, 3T3 cells treated with MSN-HA particles exhibited a

unique morphology of their cytoplasm that was mainly characterized by the presence of a large amount of vesicles filled with MSN-HA particles (Figure 7 C,D). In both samples the vesicles were delimited by a single membrane with size up to 1-2 μm in diameter (Figure 7 A-D), suggesting an internalization by endocytosis. Although most internalized MSNs were seen to be confined inside the cytoplasmic vesicles, additional MSNs particles were found free in the cytosol. In contrast, MSN-CHIT particles exhibited a significant different pattern in 3T3 cells, where they were often observed strictly associated to the external cell surfaces or forming large aggregates in the culture medium (Figure 7 E,F). Occasionally, very few MSN-CHIT particles were internalized in the cytoplasmic compartment (Figure 7 F). Moreover, in all 3T3 samples examined in this study nucleus was always found devoid of MSNs particles that remained restricted to the cytoplasmic compartment. The higher resolving power of the TEM technique highlighted the cell structure of the 3T3 cells incubated with MSNs particles. Independently of the type of functionalized MSNs used, the typical cell ultrastructure was preserved, being characterized by well developed Golgi apparatus, endoplasmic reticulum and mitochondria. No significant morphological alterations were detected when compared to control samples (see Figure S6 in Supporting Information).

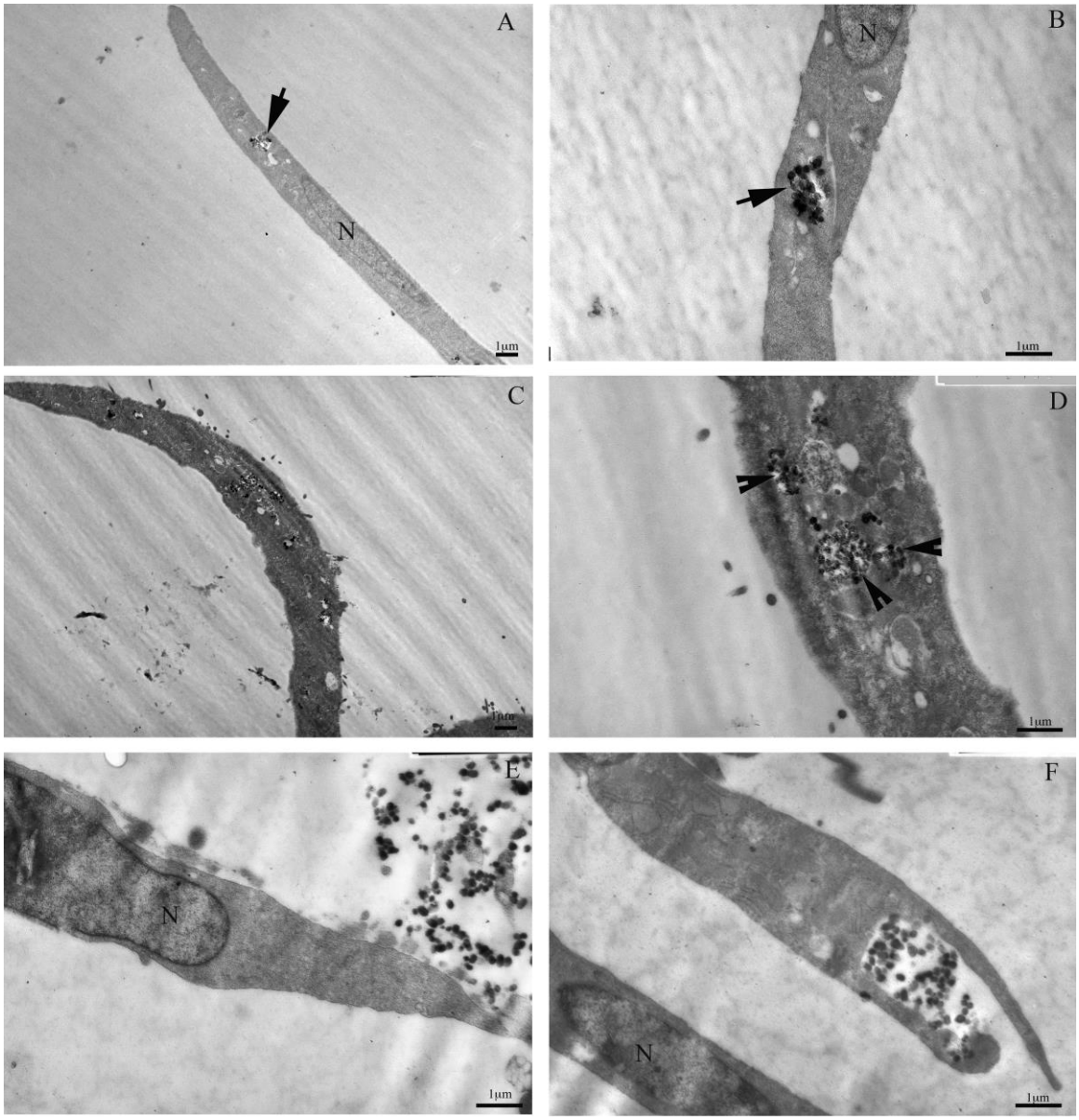

Figure 7. Electron micrographs of mouse fibroblasts 3T3 incubated for 24 hours with 100 μg/ml of MSNs, and then left to grow for other 24 hours in the culture medium before the other treatments (see par. 2.5). Panel A-B: MSM-NH_2, Panel C-D: MSN-HA, Panel E-F: MSN-CHIT. Arrows and arrowheads indicate internalized MSN-NH_2 and MSN-HA nanoparticles, respectively. N= nucleus. Additional TEM images are shown in Figure S5 (Supporting Information).

4. Discussion

As demonstrated by fluorescence microscopy, TEM images also document the significant dissimilarities in the MSNs patterns that take place in 3T3 cells following treatment with the different functionalized MSNs. The type of functionalization does not seem to affect the cellular architecture of the 3T3 mouse fibroblasts that was always well preserved and characterized by the presence of

well-developed cellular organelles. This agrees with the cell viability experiments. However, the different amounts of MSNs particles internalized in the cytoplasm of 3T3 cells following a specific MSN treatment point out the significant role of the functionalization groups of the MSNs in the cellular uptake. Both fluorescence and electron microscopy demonstrate that 3T3 cells can easily internalize MSN-HA particles much more efficiently than functionalized MSN-NH_2, suggesting a specific uptake, probably via hyaluronic acid receptor mediated endocytosis. These marked differences can be explained considering that a variety of cellular mechanisms regulate the interactions of the plasma membrane with the external materials. The endocytosis is a complex process that controls not only the internalization of extracellular materials but also the expression of specific cell-surface receptors and is deeply involved in the cellular trafficking of macromolecules and particles through the cellular compartments.[54] The unique biological properties of hyaluronic acid may account for the high biocompatibility of MSN-HA with 3T3 cells. Hyaluronic acid is an ubiquitous extracellular matrix component[55] synthesized by fibroblasts, whose interaction with its specific cell surface receptor CD44 mediates a wide range of physiological roles including cell adhesion and migration.[56]

In the present work, although the cellular mechanisms involved in MSNs internalization cannot clearly be ascertained, we may point out some considerations. The cytoplasmic vesicles visualized by electron microscopy in 3T3 cells represent the cellular organelles that participate in the intracellular trafficking of MSN particles, being one of the steps of the sorting process that takes place soon after internalization. Moreover, we observed some MSNs that are not encapsulated into vesicles, suggesting that they are able to escape from the endocytic system and translocate into the cytosol.

In contrast, MSN-CHIT particles are strictly associated to the external cellular surfaces or dispersed as large aggregates in the culture medium, and only occasionally, are able to penetrate the cells. The low rate of intracellular uptake of MSN-CHIT may be ascribed to the large size of aggregates that cannot be endocyted by 3T3 cells.

However, although their inefficiency to penetrate the cellular compartment, the peculiar pattern that MSN-CHIT particles exhibit at the electron microscopic level raises interesting questions concerning their possible biological properties and function. The MSN-CHIT affinity for the external cellular surfaces clearly depends on the specific physico-chemical properties of both chitosan and plasma membrane and could account for a potential role of chitosan in the modulation of the cellular adhesion to synthetic substrates. Lately, the growing interest in the development of biologically active coatings has led to significant improvements in the design of specific scaffolds for tissue engineering and new hypothesis are coming forth**.**[61–63] The fluorescence and TEM results highlight the morpho-functional events that characterize the interactions of artificial functionalized substrates with cell surfaces and represent a first step towards the deep understanding of the mechanisms involved in this process, but this is only the tip of the iceberg and many questions remain to be ascertained.

5. Conclusions

MSNs functionalized with amino groups (MSN-NH_2) were further functionalized at the external surface introducing a layer based on hyaluronic acid or chitosan polysaccharides, in order to obtain stimuli-responsive objects endowed with higher bioadhesion properties than non functionalized MSNs. The high level of the viability of 3T3 cells, determined through the MTS assay after a contact with the MSNs for 24 hours, was confirmed by the cell growth curve obtained through Coulter counter. The whole results clearly assess the high biocompatibility of all types of functionalized MSNs, without any significant effect due to the different functionalizations. Significant differences due to type of functionalization were instead observed in the fluorescence microscopy experiments performed with the FITC-labeled MSN-NH_2, MSN-HA and MSN-CHIT which strikingly agree with the results of TEM experiments. Using an exposure time of 24 h and 100 μg/mL of MSNs, followed by other 24 h in contact with the culture medium only, different types of interactions between MSNs and 3T3 cells can be demonstrated: MSN-NH_2, MSN-HA are easily internalized (at different extent),

whereas MSN-CHIT tend to give large aggregates dispersed in the medium or localized at external surface of the cell membranes. Both fluorescence microscopy and TEM images give clear evidence that the MSN particles are localized in the cytoplasm in the case of -NH_2 and -HA functionalizations, as shown in Figure 5 A,B and 5 C,D, as well as in Figure 7 A,B and 7 C,D. In the case of CHIT functionalization only few particles are internalized as demonstrated in Figure 5 E,F and Figure 7 E,F. These results permit to emphasize some concluding remarks: i) the importance of the external functionalization with HA allows for a very large cellular uptake: ii) the external functionalization with CHIT seems to prevent a massive uptake from 3T3 cells. In principle, it may be suggested that MSN-CHIT undergo strong interactions with the medium components that, evidently, screens the original (quite high) positive surface potential (see Table 1) thus resulting in a significant particle aggregation. In both cases the formation of a serum protein corona may play a role.[44] These results, however, do not exclude the usefulness of CHIT functionalization for delivering anticancer drugs to tumor cells (the acidic pH would favor release as a result of CHIT hydrolysis) since massive adhesion to cellular membranes occurs as clearly shown in Figure 7F. In addition, the functionalization with CHIT, that is a positively charged polyelectrolyte, may decrease the retention of MSNs within the endosome which affects the efficiency of drug release, particularly in the case of sensitive therapeutic moieties such as proteins, antibodies or DNA fragments. This was ascertained in the case of MSNs functionalized with the polyethylenimine polymer.[64]

In conclusion, the different cellular uptake observed in our *in vitro* experiments for MSNs functionalized with HA and CHIT suggests the need of further investigations not only with additional cell lines, but also a deeper evaluation of the interactions of MSNs with different dispersing media as well as the most suitable degree of functionalization. Indeed, our functionalized particles may be regarded as a stimuli-responsive platform to be tuned depending on the medium and type of cells with which particles are expected to interact.

ACKNOWLEDGMENT. MIUR, PRIN 2010-2011 grant number 2010BJ23MN-002 and Fondazione Banco di Sardegna are thanked for financial support. Prof. M. Casula is thanked for TGA measurements. Marco Sanna and Gino Paolo Asuni are thanked for experimental support.

Supporting Information Available. Additional characterizations (TGA, DLS) of MSNs samples and TEM images of control samples are available free of charge on the World Wide Web at http://pubs.acs.org.

References

(1) Baeza, A.; Colilla, M.; Vallet-Regí, M. Advances in mesoporous silica nanoparticles for targeted stimuli-responsive drug delivery. *Expert Opin. Drug Deliv.* **2015**, *12* (2), 319–337 DOI: 10.1517/17425247.2014.953051.

(2) Mamaeva, V.; Sahlgren, C.; Lindén, M. Mesoporous silica nanoparticles in medicine-recent advances. *Adv. Drug Deliv. Rev.* **2013**, *65* (5), 689–702 DOI: 10.1016/j.addr.2012.07.018.

(3) Monduzzi, M.; Lampis, S.; Murgia, S.; Salis, A. From self-assembly fundamental knowledge to nanomedicine developments. *Adv. Colloid Interface Sci.* **2014**, *205*, 48–67 DOI: 10.1016/j.cis.2013.10.009.

(4) Lebeau, B.; Galarneau, A.; Linden, M. Introduction for 20 years of research on ordered mesoporous materials. *Chem. Soc. Rev.* **2013**, *42* (9), 3661–3662 DOI: 10.1039/c3cs90005c.

(5) Gagner, J. E.; Shrivastava, S.; Qian, X.; Dordick, J. S.; Siegel, R. W. Engineering Nanomaterials for Biomedical Applications Requires Understanding the Nano-Bio Interface: A Perspective. *J. Phys. Chem. Lett.* **2012**, *3* (21), 3149–3158 DOI: 10.1021/jz301253s.

(6) Feizi, T. Oligosaccharides in molecular recognition. *Biochem. Soc. Trans.* **1988**, *16* (6), 930–934.

(7) Wang, E.; Lew, K.; Barecki, M.; Casciano, C. N.; Clement, R. P.; Johnson, W. W. Quantitative Distinctions of Active Site Molecular Recognition by P-Glycoprotein and Cytochrome P450 3A4. *Chem. Res. Toxicol.* **2001**, *14* (12), 1596–1603 DOI: 10.1021/tx010125x.

(8) Slowing, I. I.; Vivero-Escoto, J. L.; Wu, C.-W.; Lin, V. S.-Y. Mesoporous silica nanoparticles as controlled release drug delivery and gene transfection carriers. *Adv. Drug Deliv. Rev.* **2008**, *60* (11), 1278–1288 DOI: 10.1016/j.addr.2008.03.012.

(9) Wang, Y.; Zhao, Q.; Han, N.; Bai, L.; Li, J.; Liu, J.; Che, E.; Hu, L.; Zhang, Q.; Jiang, T.; et al. Mesoporous silica nanoparticles in drug delivery and biomedical applications. *Nanomedicine: NBS* **2015**, *11* (2), 313–327 DOI: 10.1016/j.nano.2014.09.014.

(10) Fu, C.; Liu, T.; Li, L.; Liu, H.; Chen, D.; Tang, F. The absorption, distribution, excretion and toxicity of mesoporous silica nanoparticles in mice following different exposure routes. *Biomaterials* **2013**, *34* (10), 2565–2575 DOI: 10.1016/j.biomaterials.2012.12.043.

(11) Kresge, C. T.; Roth, W. J. The discovery of mesoporous molecular sieves from the twenty year perspective. *Chem. Soc. Rev.* **2013**, *42* (9), 3663–3670 DOI: 10.1039/c3cs60016e.

(12) Hoffmann, F.; Cornelius, M.; Morell, J.; Fröba, M. Silica-based mesoporous organic-inorganic hybrid materials. *Angew. Chemie - Int. Ed.* **2006**, *45* (20), 3216–3251 DOI: 10.1002/anie.200503075.

(13) Böcking, D.; Wiltschka, O.; Niinimäki, J.; Shokry, H.; Brenner, R.; Lindén, M.; Sahlgren, C. Mesoporous silica nanoparticle-based substrates for cell directed delivery of Notch signalling modulators to control myoblast differentiation. *Nanoscale* **2014**, *6* (3), 1490–1498 DOI: 10.1039/c3nr04022d.

(14) Gomez-Cerezo, N.; Izquierdo-Barba, I.; Arcos, D.; Vallet-Regi, M. Tailoring the biological response of mesoporous bioactive materials. *J. Mater. Chem. B* **2015**, *3* (18), 3810–3819 DOI: 10.1039/C5TB00268K.

(15) Bhattacharyya, M. S.; Hiwale, P.; Piras, M.; Medda, L.; Steri, D.; Piludu, M.; Salis, A.; Monduzzi, M. Lysozyme adsorption and release from ordered mesoporous materials. *J. Phys. Chem. C* **2010**, *114*, 19928–19934 DOI: 10.1021/jp1078218.

(16) Steri, D.; Monduzzi, M.; Salis, A. Ionic strength affects lysozyme adsorption and release from SBA-15 mesoporous silica. *Microporous Mesoporous Mater.* **2013**, *170*, 164–172 DOI: 10.1016/j.micromeso.2012.12.002.

(17) Salis, A.; Medda, L.; Cugia, F.; Monduzzi, M. Effect of electrolytes on proteins physisorption on ordered mesoporous silica materials. *Colloids Surf. B. Biointerfaces* **2016**, *137*, 77–90 DOI: 10.1016/j.colsurfb.2015.04.068.

(18) Piras, M.; Salis, A.; Piludu, M.; Steri, D.; Monduzzi, M. 3D vision of human lysozyme adsorbed onto a SBA-15 nanostructured matrix. *Chem. Commun.* **2011**, *47* (26), 7338–7440 DOI: 10.1039/c1cc11840d.

(19) Piludu, M.; Medda, L.; Cugia, F.; Monduzzi, M.; Salis, A. Silver-Enhancement for TEM Imaging of Antibody Fragment-Gold Nanoparticles Conjugates Immobilized on Ordered Mesoporous Silica. *Langmuir* **2015**, *31* (34), 9458–9463 DOI: 10.1021/acs.langmuir.5b02830.

(20) Medda, L.; Monduzzi, M.; Salis, A. The molecular motion of bovine serum albumin under physiological conditions is ion specific. *Chem. Commun.* **2015**, *51* (30), 6663–6666 DOI: 10.1039/c5cc01538c.

(21) Salis, A.; Ninham, B. W. Models and mechanisms of Hofmeister effects in electrolyte solutions, and colloid and protein systems revisited. *Chem. Soc. Rev.* **2014**, *43* (21), 7358–7377 DOI: 10.1039/c4cs00144c.

(22) Cugia, F.; Monduzzi, M.; Ninham, B. W.; Salis, A. Interplay of ion specificity, pH and buffers: insights from electrophoretic mobility and pH measurements of lysozyme solutions. *RSC Adv.* **2013**, *3* (17), 5882 DOI: 10.1039/c3ra00063j.

(23) Medda, L.; Carucci, C.; Parsons, D. F.; Ninham, B. W.; Monduzzi, M.; Salis, A. Specific cation effects on hemoglobin aggregation below and at physiological salt concentration. *Langmuir* **2013**, *29* (49), 15350–15358 DOI: 10.1021/la404249n.

(24) Hudson, S. P.; Padera, R. F.; Langer, R.; Kohane, D. S. The biocompatibility of mesoporous silicates. *Biomaterials* **2008**, *29* (30), 4045–4055 DOI: 10.1016/j.biomaterials.2008.07.007.

(25) Vallet-Regí, M.; Izquierdo-Barba, I.; Rámila, A.; Pérez-Pariente, J.; Babonneau, F.; González-Calbet, J. M. Phosphorous-doped MCM-41 as bioactive material. *Solid State Sci.* **2005**, *7* (2), 233–237 DOI: 10.1016/j.solidstatesciences.2004.10.038.

(26) Balas, F.; Manzano, M.; Colilla, M.; Vallet-Regí, M. L-Trp adsorption into silica mesoporous materials to promote bone formation. *Acta Biomater.* **2008**, *4* (3), 514–522 DOI:

10.1016/j.actbio.2007.11.009.

(27) Vallet-Regi, M.; Ruiz-Gonzalez, L.; Izquierdo-Barba, I.; Gonzalez-Calbet, J. M. Revisiting silica based ordered mesoporous materials: medical applications. *J. Mater. Chem.* **2006**, *16* (1), 26–31 DOI: 10.1039/B509744D.

(28) Li, L.; Tang, F.; Liu, H.; Liu, T.; Hao, N.; Chen, D.; Teng, X.; He, J. In Vivo Delivery of Silica Nanorattle Encapsulated Docetaxel for Liver Cancer Therapy with Low Toxicity and High Efficacy. *ACS Nano* **2010**, *4* (11), 6874–6882 DOI: 10.1021/nn100918a.

(29) Yu, T.; Greish, K.; McGill, L. D.; Ray, A.; Ghandehari, H. Influence of Geometry, Porosity, and Surface Characteristics of Silica Nanoparticles on Acute Toxicity: Their Vasculature Effect and Tolerance Threshold. *ACS Nano* **2012**, *6* (3), 2289–2301 DOI: 10.1021/nn2043803.

(30) Meng, H.; Xue, M.; Xia, T.; Ji, Z.; Tarn, D. Y.; Zink, J. I.; Nel, A. E. Use of Size and a Copolymer Design Feature To Improve the Biodistribution and the Enhanced Permeability and Retention Effect of Doxorubicin-Loaded Mesoporous Silica Nanoparticles in a Murine Xenograft Tumor Model. *ACS Nano* **2011**, *5* (5), 4131–4144 DOI: 10.1021/nn200809t.

(31) Salvati, A.; Pitek, A. S.; Monopoli, M. P.; Prapainop, K.; Bombelli, F. B.; Hristov, D. R.; Kelly, P. M.; Aberg, C.; Mahon, E.; Dawson, K. A. Transferrin-functionalized nanoparticles lose their targeting capabilities when a biomolecule corona adsorbs on the surface. *Nat. Nanotechnol.* **2013**, *8* (2), 137–143.

(32) Guarnieri, D.; Malvindi, M. A.; Belli, V.; Pompa, P. P.; Netti, P. Effect of silica nanoparticles with variable size and surface functionalization on human endothelial cell viability and angiogenic activity. *J. Nanoparticle Res.* **2014**, *16* (2), Article ID: 2229 DOI: 10.1007/s11051-013-2229-6.

(33) Chen, Y.; Chen, H.; Shi, J. In Vivo Bio-Safety Evaluations and Diagnostic/Therapeutic Applications of Chemically Designed Mesoporous Silica Nanoparticles. *Adv. Mater.* **2013**, *25* (23), 3144–3176 DOI: 10.1002/adma.201205292.

(34) Yu, M.; Jambhrunkar, S.; Thorn, P.; Chen, J.; Gu, W.; Yu, C. Hyaluronic acid modified mesoporous silica nanoparticles for targeted drug delivery to CD44-overexpressing cancer cells. *Nanoscale* **2013**, *5* (1), 178–183 DOI: 10.1039/C2NR32145A.

(35) Medda, L.; Casula, M. F.; Monduzzi, M.; Salis, A. Adsorption of lysozyme on hyaluronic acid functionalized SBA-15 mesoporous silica: a possible bioadhesive depot system. *Langmuir* **2014**, *30* (43), 12996–13004 DOI: 10.1021/la503224n.

(36) Vasi, A. M.; Popa, M. I.; Butnaru, M.; Dodi, G.; Verestiuc, L. Chemical functionalization of hyaluronic acid for drug delivery applications. *Mater. Sci. Eng. C* **2014**, *38* (1), 177–185 DOI: 10.1016/j.msec.2014.01.052.

(37) Knudson, W.; Peterson, R. S. The hyalorunan 388 receptor: CD44. In *Chemistry and Biology of Hyalorunan*; Garg, H. G., Hales, C. A., Eds.; Elsevier Ltd: Oxford, 2004; pp 83–124.

(38) Girish, K. S.; Kemparaju, K. The magic glue hyaluronan and its eraser hyaluronidase: a biological overview. *Life Sci.* **2007**, *80* (21), 1921–1943 DOI: 10.1016/j.lfs.2007.02.037.

(39) Feng, W.; Nie, W.; He, C.; Zhou, X.; Chen, L.; Qiu, K.; Wang, W.; Yin, Z. Effect of pH-responsive alginate/chitosan multilayers coating on delivery efficiency, cellular uptake and biodistribution of mesoporous silica nanoparticles based nanocarriers. *ACS Appl. Mater. Interfaces* **2014**, *6* (11), 8447–8460 DOI: 10.1021/am501337s.

(40) Hakeem, A.; Duan, R.; Zahid, F.; Dong, C.; Wang, B.; Hong, F.; Ou, X.; Jia, Y.; Lou, X.; Xia, F. Dual stimuli-responsive nano-vehicles for controlled drug delivery: mesoporous silica

nanoparticles end-capped with natural chitosan. *Chem. Commun.* **2014**, *50* (87), 13268–13271 DOI: 10.1039/c4cc04383a.

(41) Zhao, Q.; Geng, H.; Wang, Y.; Gao, Y.; Huang, J.; Wang, Y.; Zhang, J.; Wang, S. Hyaluronic Acid Oligosaccharide Modified Redox-Responsive Mesoporous Silica Nanoparticles for Targeted Drug Delivery. *ACS Appl. Mater. Interfaces* **2014**, *6* (22), 20290–20299 DOI: 10.1021/am505824d.

(42) Senthilkumar, R.; Karaman, D. Ş.; Paul, P.; Björk, E. M.; Odén, M.; Eriksson, J. E.; Rosenholm, J. M. Targeted delivery of a novel anticancer compound anisomelic acid using chitosan-coated porous silica nanorods for enhancing the apoptotic effect. *Biomater. Sci.* **2015**, *3* (1), 103–111 DOI: 10.1039/C4BM00278D.

(43) Chen, Z.; Li, Z.; Lin, Y.; Yin, M.; Ren, J.; Qu, X. Bioresponsive hyaluronic acid-capped mesoporous silica nanoparticles for targeted drug delivery. *Chem. - A Eur. J.* **2013**, *19* (5), 1778–1783 DOI: 10.1002/chem.201202038.

(44) Shahabi, S.; Treccani, L.; Dringen, R.; Rezwan, K. Modulation of Silica Nanoparticle Uptake into Human Osteoblast Cells by Variation of the Ratio of Amino and Sulfonate Surface Groups: Effects of Serum. *ACS Appl. Mater. Interfaces* **2015**, *7*, 13821–13833 DOI: 10.1021/acsami.5b01900.

(45) Slowing, I.; Trewyn, B. G.; Lin, V. S.-Y. Effect of Surface Functionalization of MCM-41-Type Mesoporous Silica Nanoparticles on the Endocytosis by Human Cancer Cells. *J. Am. Chem. Soc.* **2006**, *128* (46), 14792–14793 DOI: 10.1021/ja0645943.

(46) Slowing, I. I.; Trewyn, B. G.; Lin, V. S.-Y. Mesoporous Silica Nanoparticles for Intracellular Delivery of Membrane-Impermeable Proteins. *J. Am. Chem. Soc.* **2007**, *129* (28), 8845–8849 DOI: 10.1021/ja0719780.

(47) Luft, J. H. Improvements in epoxy resin embedding methods. *J. Biophys. Biochem. Cytol.* **1961**, *9* (2), 409–414.

(48) Ravikovitch, P. I.; Wei, D.; Chueh, W. T.; Haller, G. L.; Neimark, a. V. Evaluation of pore structure parameters of MCM-41 catalyst supports and catalysts by means of nitrogen and argon adsorption. *J. Phys. Chem. B* **1997**, *101* (19), 3671–3679 DOI: 10.1021/jp9625321.

(49) Salis, A.; Casula, M. F.; Bhattacharyya, M. S.; Pinna, M.; Solinas, V.; Monduzzi, M. Physical and Chemical Lipase Adsorption on SBA-15: Effect of Different Interactions on Enzyme Loading and Catalytic Performance. *ChemCatChem* **2010**, *2* (3), 322–329 DOI: 10.1002/cctc.200900288.

(50) Harris, J. R.; Roos, C.; Djalali, R.; Rheingans, O.; Maskos, M.; Schmidt, M. Application of the negative staining technique to both aqueous and organic solvent solutions of polymer particles. *Micron* **1999**, *30* (4), 289–298 DOI: 10.1016/S0968-4328(99)00034-7.

(51) Ponomarev, A. P.; Molchanova, A. I.; Uziumov, V. L. [Effect of the contrast conditions using solutions of phosphotungstic acid on the electron microscopic image of the foot-and-mouth disease virus]. *Vopr Virusol* **1979**, No. 5, 470–476.

(52) Silverman, L.; Glick, D. The reactivity and staining of tissue proteins with phosphotungstic acid. *J. Cell Biol.* **1969**, *40* (3), 761–767.

(53) Bancos, S.; Tsai, D.-H.; Hackley, V.; Weaver, J. L.; Tyner, K. M. Evaluation of Viability and Proliferation Profiles on Macrophages Treated with Silica Nanoparticles In Vitro via Plate-Based, Flow Cytometry, and Coulter Counter Assays. *ISRN Nanotechnol.* **2012**, *2012*, Article ID 454072 DOI: 10.5402/2012/454072.

(54) Doherty, G. J.; McMahon, H. T. Mechanisms of endocytosis. *Annu. Rev. Biochem.* **2009**, *78*, 857–902 DOI: 10.1146/annurev.biochem.78.081307.110540.

(55) Necas, J.; Bartosikova, L.; Brauner, P.; Kolar, J. Hyaluronic acid (hyaluronan): A review. *Vet. Med.* **2008**, *53* (8), 397–411.

(56) Jordan, A. R.; Racine, R. R.; Hennig, M. J. P.; Lokeshwar, V. B. The Role of CD44 in Disease Pathophysiology And Targeted Treatment. *Front. Immunol.* **2015**, *6*, Article 182 DOI: 10.3389/fimmu.2015.00182.

(57) Johnson, P.; Maiti, A.; Brown, K. L.; Li, R. A role for the cell adhesion molecule CD44 and sulfation in leukocyte-endothelial cell adhesion during an inflammatory response? *Biochem. Pharmacol.* **2000**, *59* (5), 455–465 DOI: 10.1016/s0006-2952(99)00266-x.

(58) Ahrens, T.; Assmann, V.; Fieber, C.; Termeer, C. C.; Herrlich, P.; Hofmann, M.; Simon, J. C. CD44 is the Principal Mediator of Hyaluronic-Acid-Induced Melanoma Cell Proliferation. *J. Invest. Dermatol.* **2001**, *116* (1), 93–101.

(59) Song, Y.; Feng, D.; Shi, W.; Li, X.; Ma, H. Parallel comparative studies on the toxic effects of unmodified CdTe quantum dots, gold nanoparticles, and carbon nanodots on live cells as well as green gram sprouts. *Talanta* **2013**, *116*, 237–244 DOI: 10.1016/j.talanta.2013.05.022.

(60) Song, Y.; Wang, Z.; Li, L.; Shi, W.; Li, X.; Ma, H. Gold nanoparticles functionalized with cresyl violet and porphyrin via hyaluronic acid for targeted cell imaging and phototherapy. *Chem. Commun.* **2014**, *50* (99), 15696–15698 DOI: 10.1039/C4CC07565J.

(61) Kornu, R.; Smith, R. L.; Maloney, W. J.; Kelly, M. A. Osteoblast adhesion to orthopaedic implant alloys: Effects of cell adhesion molecules and diamond-like carbon coating. *J. Orthop. Res.* **1996**, *14* (6), 871–877 DOI: 10.1002/jor.1100140605.

(62) El-Ghannam, A.; Ducheyne, P.; Shapiro, I. M. Effect of serum proteins on osteoblast adhesion to surface-modified bioactive glass and hydroxyapatite. *J. Orthop. Res.* **1999**, *17* (3), 340–345 DOI: 10.1002/jor.1100170307.

(63) Decuzzi, P.; Ferrari, M. Modulating cellular adhesion through nanotopography. *Biomaterials* **2010**, *31* (1), 173–179 DOI: 10.1016/j.biomaterials.2009.09.018.

(64) Li, X.; Chen, Y.; Wang, M.; Ma, Y.; Xia, W.; Gu, H. A mesoporous silica nanoparticle - PEI - fusogenic peptide system for siRNA delivery in cancer therapy. *Biomaterials* **2013**, *34* (4), 1391–1401 DOI: 10.1016/j.biomaterials.2012.10.072.

Table of Contents

Mesoporous Silica Nanoparticles Functionalized with Hyaluronic Acid and Chitosan Biopolymers. Effect of Functionalization on Cell Internalization

Andrea Salis, Maura Fanti, Luca Medda, Valentina Nairi, Francesca Cugia, Marco Piludu, Valeria Sogos, and Maura Monduzzi